by laser spectroscopy

B. Roussière[1], L. Cabaret[2], J.E. Crawford[3], S. Essabaa[1], V. Fedoseyev[4], W. Geithner[5], J. Genevey[6], M. Girod[7], G. Huber[5], R. Horn[5], S. Kappertz[5], J. Lassen[5], F. Le Blanc[1], J.K.P. Lee[3], G. Le Scornet[8], J. Lettry[9], V. Mishin[4], R. Neugart[5], J. Obert[1], J. Oms[1], A. Ouchrif[1], S. Péru[7], J. Pinard[2], H. Ravn[9], J. Sauvage[1], D. Verney[1] and the ISOLDE collaboration

1 Institut de Physique Nucléaire, IN2P3-CNRS, 91406 Orsay Cedex, France
2 Laboratoire Aimé Cotton, 91405 Orsay Cedex, France
3 Physics Department, McGill University, H3A2T8 Montréal, Canada
4 Institute of Spectroscopy, Troitsk, Russia
5 Institut für Physik der Universität Mainz, 55099 Mainz, Germany
6 Institut des Sciences Nucléaires, IN2P3-CNRS, 38026 Grenoble Cedex, France
7 Service de Physique et Techniques Nucléaires, DAM-CEA, BP 12, 91680 Bruyères-le-Châtel, France
8 Centre de Spectrométrie Nucléaire et de Spectrométrie de Masse, IN2P3-CNRS, 91405 Orsay Cedex, France
9 EP Division, CERN, 1211 Geneva 23, Switzerland

Abstract

Laser spectroscopy measurements have been performed on neutron rich tin isotopes using the COMPLIS experimental setup. The nuclear charge radii of the even-even isotopes from A = 108 to 132 are compared to the results of macroscopic and microscopic calculations. The improvements and optimizations needed to perform the isotope shift measurement on ^{134}Sn are presented.

EXT-2001-050
28/08/2001

1. Introduction

The study of optical transitions through long isotopic chains is a very useful tool to determine the global properties of the ground and isomeric states of nuclei far from stability. It enables the measurement of *i)* the change in the mean square charge radius ($\delta <r_c^2>$) from the isotope shift, and *ii)* the magnetic moment (μ) and the spectroscopic quadrupole moment (Q_S) from the hyperfine structure. This type of measurement requires high resolution laser spectroscopy. For tin isotopes, the atomic transition used has a wavelength of 286.4 nm ($5p^2\ ^3P_0 \rightarrow 5p6s\ ^3P_1$) corresponding to a frequency of 10^6 GHz. For this transition, the isotope shift between two adjacent masses is around 100 MHz [1], which means that the effect we want to measure is of the order of 10^{-7}.
In this paper, we present the first laser spectroscopy results obtained on the neutron rich tin isotopes. First, the motivation for this work will be indicated and second the experimental methods used will be described. Then the charge radii of the even-even tin isotopes will be compared to the results of macroscopic and microscopic theoretical models. Finally the future prospects of this study will be discussed.

2. The physics case

Magic and doubly magic nuclei are of great interest in nuclear physics. The properties of the stable doubly magic nuclei (e.g. binding energy, neutron separation energy, radius)

have been widely used to determine the parameters of the effective nuclear interactions used in the mean field calculations. The proton-magic tin isotope series contains the doubly magic nucleus ^{132}Sn which is located far from stability. Thus observables in this nucleus, such as radius, can be used to improve the nuclear effective interaction in order to get better predictions for nuclei far from stability. Since the radii of the stable tin isotopes have been determined from muonic atom experiments [2], the measurement of the isotope shift in tin isotopes gives access to the tin radii, and especially to the radius of ^{132}Sn.

Figure 1 shows the energy of the first excited 2^+ state in the even-even nuclei of some isotopic series near the magic proton number Z = 50, as well as the change in the mean square charge radius already measured. The energy of this 2^+ state indicates if the nucleus is deformed or spherical: one expects a 2^+ state located at high energy in spherical nuclei and at low energy in deformed nuclei. Moreover a nucleus is all the more difficult to deform as its nucleon number is close to closed shells, in this region Z = 50 for protons and N = 50 or 82 for neutrons. For Cd and Te which have two protons less or more than Sn (Z =50), when the neutron number increases up to N = 82, the energy of the 2^+ state first decreases slightly, then is almost constant, and after that increases. In Ba and Xe, for which the proton numbers are farther from Z = 50, the 2^+ energy shows a minimum for the middle of the neutron shell indicating a maximum of the deformation, then its energy increases with N up to N = 82. In the spherical proton-magic tin isotopes, the 2^+ energy is quite constant between N = 52 and 80 and very similar to the values observed

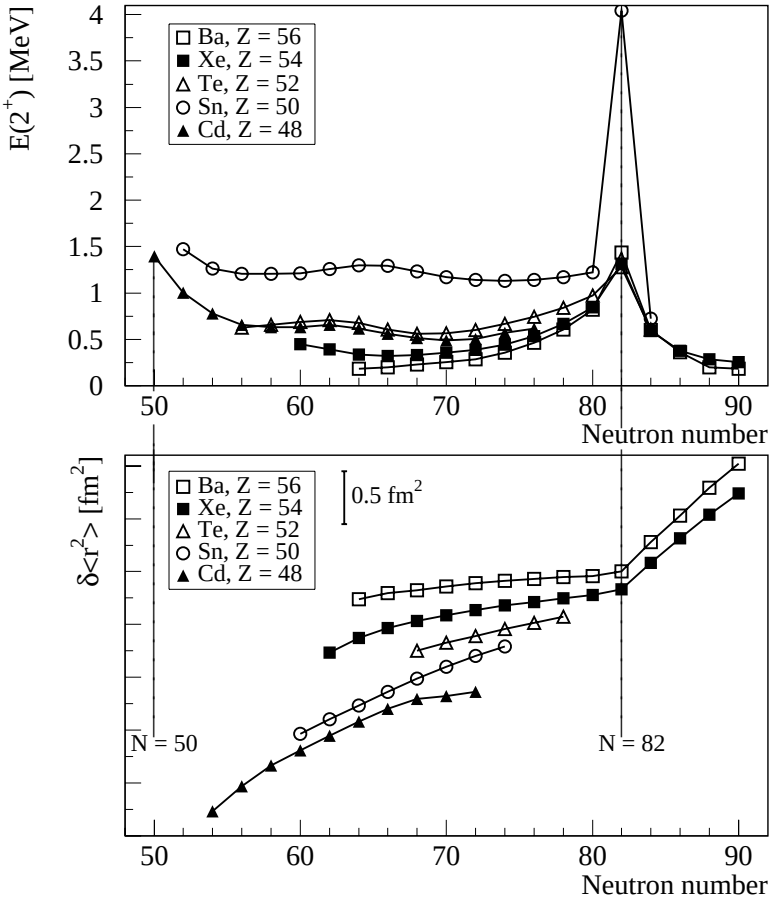

Figure 1: Energy of the first excited 2^+ states and $\delta <r_c^2>$ in some isotopic series near Z = 50.

in the N = 82 magic nuclei of the neighbouring isotopic series. The sharp increase of the 2^+ energy at N = 82 shows the strong stiffness of the doubly magic nucleus ^{132}Sn.
As regards now the behaviour of the $\delta <r_c^2>$ in these isotopic series, one can note that in Ba and Xe, the crossing of the N = 82 closed neutron shell results in a $\delta <r_c^2>$ slope change, indicating that the magic nuclei are spherical and that the deformation is increasing when the neutron number moves away from the N = 82 magic number. Moreover, from Ba to Sn, when Z decreases down to the proton magic number Z = 50, the slope of the $\delta <r_c^2>$ curve increases indicating a decrease of the deformation change. Thus one expects that, in the spherical Sn isotopes, no slope change will occur in the $\delta <r_c^2>$ curve at N = 82. However, as a kink has been observed at N = 128 (neutron closed shell) in the magic Pb nuclei (Z = 82), it remains to be seen whether there is a kink at N = 82 in the proton magic Sn nuclei.

3. Experimental procedure

3.1. Yields of the neutron rich Sn nuclei

The neutron rich tin nuclei have been obtained at ISOLDE by fission reactions, in an uranium carbide target, induced by the 1 GeV proton beam delivered by the CERN-PS-Booster. This target is associated either with the MK5 hot plasma ion source designed for the ionization of low volatility elements or with a laser ion source tuned for tin. Figure 2 shows the very similar tin yields obtained with both types of ion source. It is worth noting that, with the hot plasma source, many other elements are ionized like In, Cd, Sb, Te, I and Cs, and for instance at A = 132 tin represents only 0.24% of the observed nuclei. With the laser ion source, Cs is also ionized, probably by the surface ionization

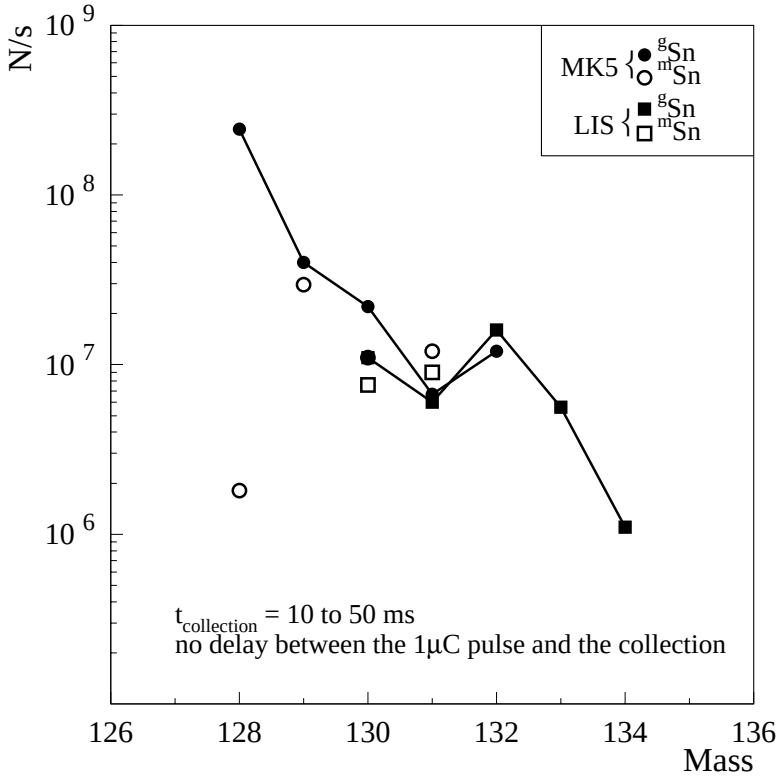

Figure 2: Yields of tin obtained with the hot plasma and laser ion sources.

mechanism. The Cs yields are high: for instance at A = 130, Cs production is 50 times that of tin, and even higher than that observed with the hot plasma ion source. These various isobaric contaminations have to be taken into account to determine which ion source has to be used depending on the setup chosen to perform laser spectroscopy measurements. Indeed three setup are available at ISOLDE: COLLAPS, COMPLIS and the laser ion source. The laser ion source [3] has an excellent efficiency due to its high laser repetition rate (10 kHz); the optical resolution (some GHz) gives elemental selectivity for most elements but it is not high enough to perform isotope shift measurements in the tin nuclei. COLLAPS [4], designed to perform collinear laser spectroscopy on fast atomic beams, has an excellent frequency resolution ($\sim$ 65 MHz) but works best with isobar-free beams, which excludes the use of the hot plasma ion source. But even with the laser ion source, the great amount of Cs isobars could give rise to a fluorescent light and thus to a continuous background noise reducing the detector sensitivity. COMPLIS, designed originally for high resolution studies on refractory or daughter elements, was not an obvious choice for experiments on tin. However, it is in fact competitive, since the hot plasma ion source, whose Cs yield is lower than that of the laser ion source, can be used. Up to now, the only experimental data from laser spectroscopy on the neutron rich Sn isotopes have been obtained using COMPLIS.

3.2. Laser spectroscopy measurements

The COMPLIS experimental setup has been described elsewhere in detail [5]. The tin ions delivered at 60 kV by ISOLDE enter the COMPLIS incident beam line, are decelerated to 1 kV and implanted in the first atomic layers of a graphite disk. The collected atoms are desorbed by a pulsed Nd:YAG laser focused beam at 532 nm. Some microseconds later, two synchronized lasers are fired to selectively ionize the tin atoms by two resonant laser excitations into the continuum. Spectroscopic information is obtained by scanning the first laser excitation step at 286.4 nm ($5p^2\ ^3P_0 \rightarrow 5p6s\ ^3P_1$ transition) supplied by a single mode continuously tunable pulsed dye laser [6]. The frequency of this laser is monitored using a Fabry-Perot interferometer, an iodine absorption cell and a lambdameter to have precise relative and absolute frequency calibration. The second excitation is into a broad auto-ionizing level at a wavelength of 410 nm. When the frequency of the first excitation step corresponds to a resonant transition, the tin atoms are excited and ionized. Then the ions are accelerated, deflected to the COMPLIS emergent line by a magnet and finally detected by microchannel plates with a time of flight mass-analysis. The frequency spectrum of the isotope under study is recorded simultaneously with that of a stable or long-lived tin isotope previously collected on the graphite disk and used as a reference for the optical isotope shift determination. The stable tin ions, provided by a stable-beam injector linked to the COMPLIS incident beam line, are also used to determine the optimal conditions for the desorption and ionization before the experiment. The tin isotopes studied in ours experiments range from A = 125 up to 132.

3.2.1. The COMPLIS running modes

Two running modes are available with COMPLIS: the collection-desorption mode and the step-by-step mode.

In the collection-desorption mode, the measurement starts by the collection of the isotope under study. During about a quarter of an hour, the ions delivered by ISOLDE are collected on the slowly rotating graphite disk. Then the disk turns back to its initial

position and starts rotating again with the same velocity as during the collection while the Nd:YAG pulses desorb the surface-implanted ions and the frequency scan is performed. Thus there is a waiting time, equal to the collection time, between the collection of the ions and the laser measurement. This running mode is suitable for the long-lived isotopes ($T_{\frac{1}{2}} \gtrsim 5$ m).

In the step-by-step mode, the ion collection is performed at a fixed position of the graphite disk during some ten seconds (one or several PS-Booster macrocycles). Then, in order to optimize the overlap between the collection spot (width $\sim$ 1 mm) and the desorption spot (width ~ 50 μm), the disk turns around this position to explore the whole implanted spot during the measurement, i.e. the desorption and the ionization at a given frequency of the excitation step. After the frequency of the excitation step is changed, the cycle collection-measurement is repeated to scan the whole chosen frequency range. This second running mode is used for the short-lived isotopes or those with low yield since it allows the accumulation of the isotopes under study before the laser measurement.

The comparison of the hyperfine spectra obtained using both running modes allows us to distinguish between the hyperfine transitions corresponding to the ground and isomeric states provided their half-lives are different. In the spectrum obtained in the collection-desorption mode shown in fig. 3a, the transitions corresponding to the ground state of ^{125}Sn have high intensity whereas those corresponding to the isomeric state of shorter half-life are weak. On the contrary, in the spectrum obtained in the step-by-step running mode (fig. 3b), all the hyperfine transitions have roughly the same intensity, because in this running mode there is no waiting time between the collection and the measurement, thus the shorter half-life isomer has not yet decayed.

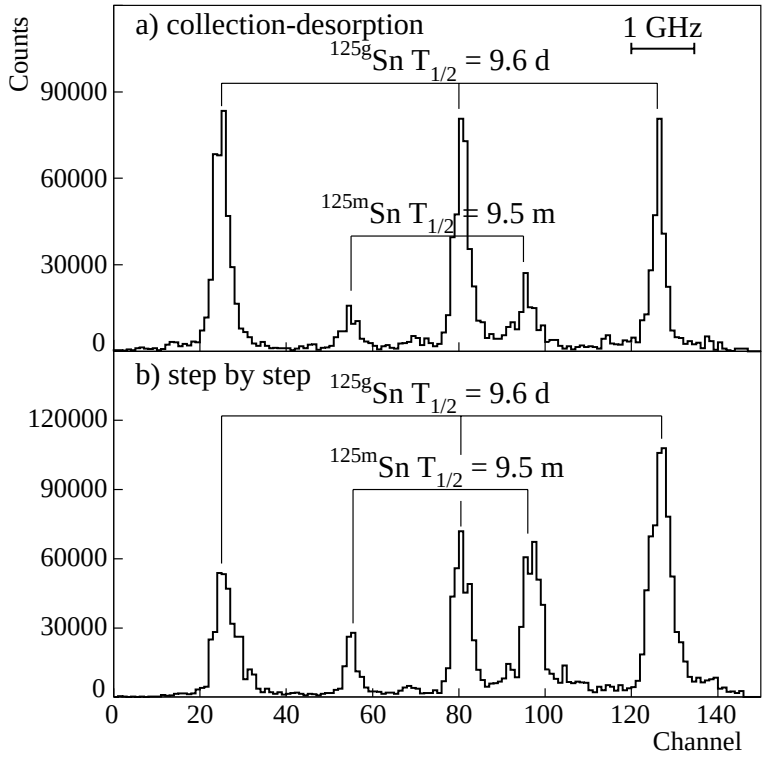

Figure 3: Hyperfine spectra of the two isomers of ^{125}Sn obtained with the collection-desorption (a) and step-by-step (b) running modes.

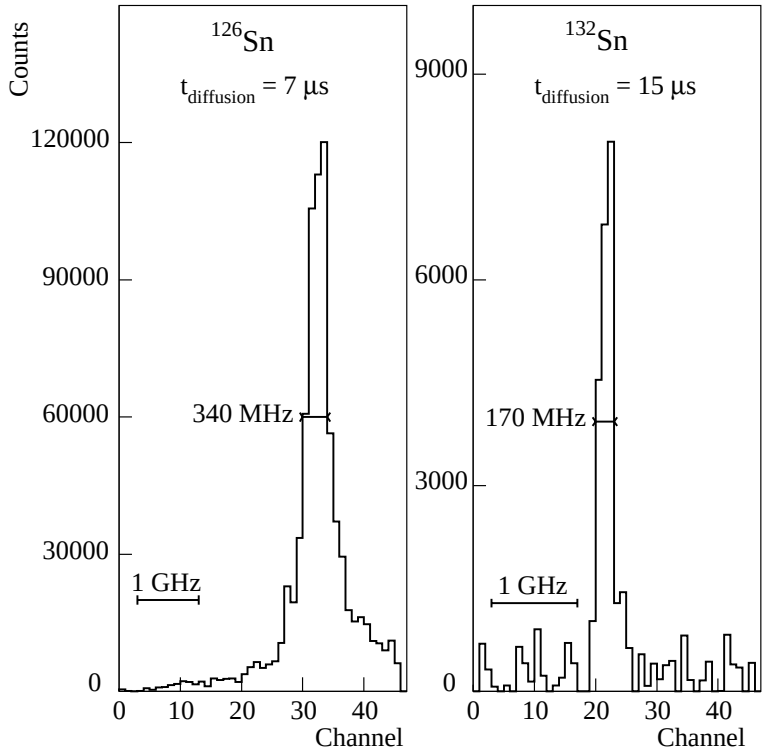

Figure 4: Influence of the diffusion time on the frequency resolution.

3.2.2. The frequency resolution

The frequency resolution obtained with COMPLIS is limited mainly by the Doppler broadening related to the dispersion in the desorbed atom velocity component parallel to the direction of the laser beam used for the excitation step. If we define x, y and z, a system of three orthogonal axes, x being the direction orthogonal to the graphite disk, y the direction of the ionization laser beam and z the direction of the excitation step laser beam, one can show [7] that the frequency resolution can be written as: $\frac{\Delta\nu}{\nu} = \frac{a}{c \times t_d}$, where a is the width of the ionization beam along z, c the speed of light in vacuum and t_d the diffusion time, i.e. the time between the desorption and the ionization.

Figure 4 shows the frequency spectra obtained for ^{126}Sn and ^{132}Sn when the diffusion time was fixed to 7 μs in the first case and to 15 μs in the second case. Increasing the diffusion time by a factor of 2 results in an improvement of the frequency resolution by a factor of 2. It is worth noting that the resolution obtained for ^{132}Sn is the best that we have ever obtained and it is excellent for such a kind of experimental setup. Indeed, we have to make a compromise between resolution and efficiency since, for a given experimental condition defined by a the width of the ionization beam and d the distance along x between the collection disk and the excitation and ionization laser beam crossing, an increase of the diffusion time results in a gain in frequency resolution but also in a loss in efficiency.

4. Experimental results and discussion

The isotope shift contains three contributions: the normal mass shift (NMS), the specific mass shift (SMS) and the field shift (FS). The field shift arises when the transition involves an electron s or $p_{\frac{1}{2}}$, i.e. an electron with a non-vanishing probability to be inside the nucleus. The field shift can be written as : $\Delta\nu_{FS} = \mathrm{F} \times \lambda$, with F an electronic

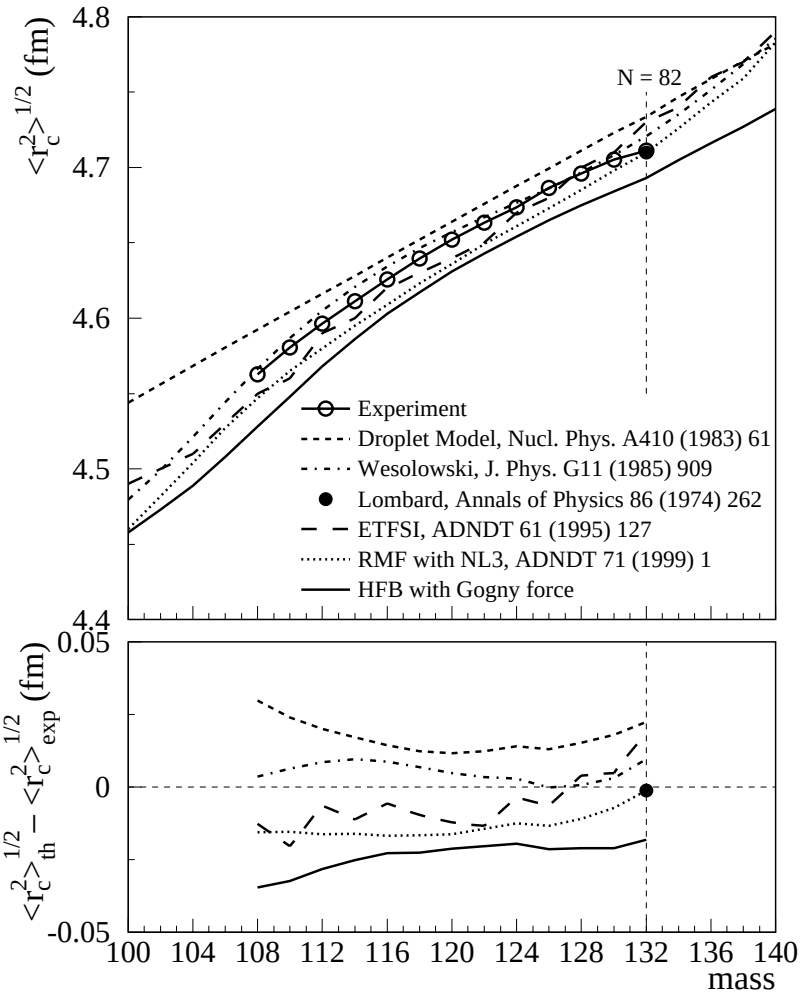

Figure 5: Comparison of the experimental charge radius in tin isotopes with predictions of various models.

factor and λ a nuclear factor related to $\delta <r_c^2>$, $\lambda = K \times \delta <r_c^2>$ [8]. The normal mass shift is easy to calculate, and in order to evaluate the specific mass shift and the F factor, we have made a King plot using the precise results available for the numerous stable tin isotopes : the $\delta\nu^{AA'}$ obtained by laser spectroscopy for the 286.4 nm transition [1] and the $\delta <r_c^2>$ obtained from muonic atom experiments [2]. This analysis led to F = 3.29±0.30 GHz/fm^2 and $\Delta\nu_{SMS}^{AA'} = -2.28 \times \Delta\nu_{NMS}^{AA'}$. Moreover, since the muonic atom experiments give access to the nuclear charge radius of the stable tin isotopes, we have extracted from the $\delta <r_c^2>$ measurements the radius of all the neutron rich tin isotopes up to ^{132}Sn.

Figure 5 shows the charge radius of the even-even tin isotopes from A = 108 up to 132. Theoretical values obtained using macroscopic or microscopic approaches are also indicated in this figure. Concerning the macroscopic approaches, the well known spherical droplet model [9] gives radius values systematically higher than the experimental ones. The Wesolowski formula [10] takes into account neutron shell effects related to the neutron occupation number between the N = 50 and N = 82 closed shells. These neutron shell effects give rise to a parabolic behaviour of the radius which is in quite good agreement with the experiment. Concerning now the microscopic calculations, the first value has been given by Beiner and Lombard [11] for ^{132}Sn. It has been obtained in the frame of an extension of the Brueckner formulation of the energy density formalism tak-

ing into account shell structure effects. It is in perfect agreement with the experimental value. It would be interesting to extend this calculation to the other tin isotopes in order to know if this excellent theory-experiment agreement is obtained all along the isotopic series. The next microscopic approach is the Extended Thomas Fermi plus Strutinsky Integral (ETFSI) method [12] that is a semi classical approximation of the Hartree-Fock method using the Skyrme SkSC4 effective interaction and including Strutinsky shell corrections. The agreement with the experimental values is quite good. The values obtained by the relativistic mean-field theory with the NL3 effective interaction [13] are also in good agreement with the experiment. The last theoretical values reported in fig. 5 have been obtained by the Hartree-Fock Bogolyubov static calculations using the Gogny force; in this case, the calculated radii are systematically below the experimental values, the general trend, however, is quite well reproduced. One can wonder whether this systematic difference between the theoretical and experimental $<r_c^2>$ values is reduced when dynamic calculations are performed.
The differences between these various theoretical values and the experimental charge radii are also reported in fig. 5. In all cases, they are smaller than 0.8%. It is worth noting that the microscopic approaches give a theory-experiment agreement as good as the macroscopic approaches. However, the behaviour of the charge radius beyond A = 132 remains an open question.

5. Future prospects

5.1. Measurements beyond ^{132}Sn

Improvements and optimization of the COMPLIS setup are needed and under way for isotope shift measurement beyond ^{132}Sn. For example, the ^{134}Sn yield is $\sim 10^6$ atoms/s, the Cs isotopes are $\sim$ 100 times more produced and the half-life of ^{134}Sn is very short ($T_{\frac{1}{2}} = 1.1$ s). Under these conditions, no accumulation of ^{134}Sn is possible and the step-by-step running mode cannot be used. Therefore the laser measurement has to be performed simultaneously with the collection. This requires a maximum overlap between the collection spot and the YAG desorption spot. The present overlap is poor since the widths of the collection and YAG desorption spots are $\sim$ 1 mm and $\sim$ 50 μm, respectively. To increase this overlap, we plan to use a multiple slit transmission grating, placed near the lens focusing the desorption laser beam, in order to diffract this laser beam and obtain several desorption spots on the focal plane. A first test has been done using slits of 0.3 mm width at 1.4 mm intervals, giving five desorption spots of approximately equal intensity in the collection zone. Figure 6 shows two hyperfine spectra recorded, for ^{131}Sn, with and without the slits. One can note that with the slits, the statistics is better indicating that the efficiency has been improved, with slight loss in frequency resolution due to the increased desorption zone increasing the Doppler broadening.

The other major improvement that we want to bring to the COMPLIS setup is to add a pulsed high voltage deflector in the emergent line in order to prevent the ions having a mass around A = 130 and created in the desorption process (and thus some 10 μs before the ions under study) to reach the detector. We hope, in that way, to improve the detector efficiency for the ions of interest, to reduce the parasitic noise and to obtain an improved transmission in the COMPLIS emergent beam line.

5.2. The hyperfine spectra of the odd tin isotopes

The hyperfine spectra of the odd tin isotopes exhibit only five lines instead of the six

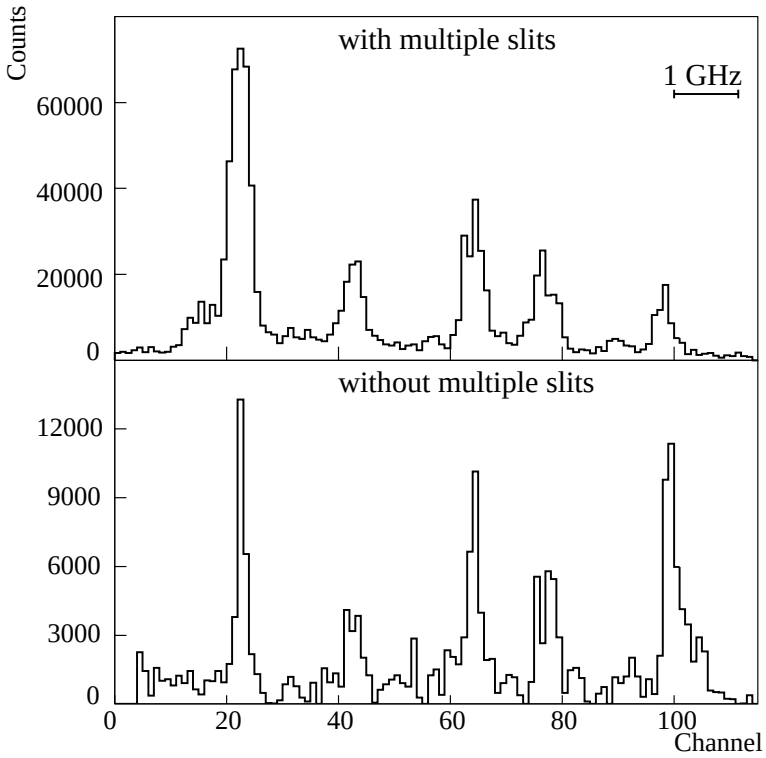

Figure 6: Hyperfine spectra of ^{131}Sn.

expected from both spin values $I^{\pi} = \frac{11}{2}^{-}$ and $\frac{3}{2}^{+}$ attributed to the ground and isomeric states (see figs. 3 and 6). Either one of the hyperfine transition corresponding to the isomeric state is merged into a transition belonging to the ground state, or the spin of one of these states is not $\frac{3}{2}$ but $\frac{1}{2}$ giving rise to two hyperfine transitions only. The analysis of the spectra is in progress and at the moment seems to confirm the first hypothesis. Direct experimental answers could be obtained by either performing measurements with COLLAPS which has an excellent frequency resolution and thus could separate the mixed resonant transitions, or using SIINODE (Séparation Isomérique et Isobarique des NOyaux DEscendants) which is an upgrading, presently under construction, to use COMPLIS as an isomeric separator.

The chamber located at the end of the COMPLIS emergent line and containing the microchannel plate detector will be replaced by a set of chambers that allows either the detection of the ions with a microchannel plate detector or, when removed, the collection of the ions on a tape. This tape can be moved in front of a Ge detector to perform γ-spectroscopy measurements. Using SIINODE for the odd tin isotopes, we will set the excitation step laser to a frequency corresponding to a given resonant transition and we will be able to attribute firmly this hyperfine transition to one of the ground or isomeric state or to both states, depending on the emitted γ-rays observed.

References

[1] M. Anselment *et al.*, Phys. Rev. **C34**, 1052 (1986).
[2] C. Piller *et al.*, Phys. Rev. **C42**, 182 (1990).
[3] J. Lettry *et al.*, Rev. Sci. Instr. **69**, 761 (1998).
[4] R. Neugart, Inst. Phys. Conf. Ser. **132**, 133 (1992).
[5] J. Sauvage *et al.*, Hyperfine Interactions **129**, 303 (2000).
[6] J. Pinard and S. Liberman, Opt. Comm. **20**, 334 (1977).

[7] J. Pinard *et al.*, Proceedings of the 3^{rd} International Workshop on Hyperfine Structure and Nuclear Moments of Exotic Nuclei by Laser Spectroscopy, Poznań, Poland, February 3-5, 1997.
[8] G. Torbhom *et al.*, Phys. Rev. **A31**, 2038 (1985).
[9] W.D. Myers and K.H. Schmidt, Nucl. Phys. **A410**, 61 (1983).
[10] E. Wesołowski, J. Phys. **G11**, 909 (1985).
[11] M. Beiner and R.J. Lombard, Annals of Physics **86**, 262 (1974).
[12] Y. Aboussir *et al.*, Atomic Data and Nuclear Data Tables **61**, 127 (1995).
[13] G.A. Lalazissis *et al.*, Atomic Data and Nuclear Data Tables **71**, 1 (1999).